JOURNAL OF VIROLOGY, Aug. 2004, p. 8229–8237 Vol. 78, No. 15
0022-538X/04/$08.00+0 DOI: 10.1128/JVI.78.15.8229–8237.2004

Progression or Resolution of Coxsackievirus B4-Induced Pancreatitis: a Genomic Analysis†

Stephanie E. Ostrowski,[1]‡ Andrew A. Reilly,[2] Doris N. Collins,[3] and Arlene I. Ramsingh[1,3]*

Department of Biomedical Sciences[1] and Department of Biometry and Statistics,[2] School of Public Health, State University of New York at Albany, Albany, New York 12237, and Wadsworth Center, New York State Department of Health, 120 New Scotland Avenue, Albany, New York 12208[3]

Received 21 January 2004/Accepted 28 April 2004

Group B coxsackieviruses are associated with chronic inflammatory diseases of the pancreas, heart, and central nervous system. Chronic pancreatitis, which can develop from acute pancreatitis, is considered a premalignant disorder because it is a major risk factor for pancreatic cancer. To explore the genetic events underlying the progression of acute to chronic disease, a comparative analysis of global gene expression during coxsackievirus B4-induced acute and chronic pancreatitis was undertaken. A key feature of acute pancreatitis that resolved was tissue regeneration, which was accompanied by increased expression of genes involved in cell growth, inhibition of apoptosis, and embryogenesis and by increased division of acinar cells. Acute pancreatitis that progressed to chronic pancreatitis was characterized by lack of tissue repair, and the expression map highlighted genes involved in apoptosis, acinoductular metaplasia, remodeling of the extracellular matrix, and fibrosis. Furthermore, immune responses appeared skewed toward development of alternatively activated (M2) macrophages and T helper 2 (Th2) cells during disease that resolved and toward classically activated (M1) macrophages and Th1 cells during disease that progressed. Our hypothesis is that growth and differentiation signals coupled with the M2/Th2 milieu favor acinar cell proliferation, while diminished growth signals and the M1/Th1 milieu favor apoptosis of acinar cells and remodeling/proliferation of the extracellular matrix, resulting in fibrosis.

The group B coxsackieviruses are associated with chronic inflammatory diseases of the pancreas (insulin-dependent diabetes mellitus and idiopathic chronic pancreatitis), heart (dilated cardiomyopathy), and central nervous system (12). Efforts to elucidate the mechanisms by which these viruses cause disease have focused on identifying the molecular determinants of viral virulence and understanding the immune response to infection. The molecular determinants of viral virulence for the group B coxsackieviruses are distinct, suggesting that these viruses induce disease via diverse mechanisms. For coxsackievirus B3 (CVB3), determinants of attenuation and virulence have been identified in the 5′ untranslated region (42) and in VP2 (21). For CVB4, Thr-129 of VP1 is a major determinant of virulence (11). The precise mechanism by which the viral molecular determinants cause tissue injury is not clear. During coxsackievirus B infection, both virus-induced cytopathology and immunopathological mechanisms have been implicated in mediating tissue injury (12, 36).

Our mouse model uses two serologically indistinguishable variants of the CVB4 serotype that cause acute and chronic pancreatitis reminiscent of clinical disease. The CVB4-P variant induces a transient, acute disease which shares pathological features (edema and inflammation) (34) with acute, interstitial pancreatitis in humans (9). The CVB4-V variant induces a severe, acute disease which progresses to chronic pancreatitis. CVB4-V-induced chronic pancreatitis (34) shares several morphological features with clinical chronic pancreatitis (25), including prolonged inflammation, extensive loss of exocrine tissue, acinoductular metaplasia, edema, and fibrosis. Furthermore, both CVB4-V-induced chronic pancreatitis and clinical chronic pancreatitis result in the development of exocrine pancreatic insufficiency, leading to malnutrition and weight loss (35, 25). A major difference between the two viral infections is that pancreatic tissue damage is resolved after CVB4-P infection but is permanent after CVB4-V infection. Again, this distinction is observed in clinical disease, since tissue damage can resolve during acute pancreatitis, while damage is irreversible in chronic pancreatitis. The current study focused on a correlative analysis of gene expression maps of CVB4-induced pancreatitis with pathological changes occurring in the pancreas.

MATERIALS AND METHODS

Cells, viruses, and mice. The passage histories of CVB4-P and CVB4-V have been described (16). Viral infectivity was assessed by plaque assay with LLC-MK2(D) cells. BALB/cByJ mice were bred and maintained in the Animal Core Facility of the Wadsworth Center (Albany, N.Y.). Eight-week-old female mice were infected intraperitoneally with 10^4 PFU of CVB4-P. Because of the virulent phenotype of CVB4-V, a titration (10, 50, and 100 PFU) was done to identify the lowest dose of virus that resulted in consistent pathological changes in the pancreas during a 2-week period. For CVB4-V infections, a dose of 50 PFU was used. Because CVB4-V-infected mice develop exocrine pancreatic insufficiency (35), mice were given supplements of pancreatic enzymes (1 mg of pancreatin per ml) and sucrose (10%) in their drinking water to minimize morbidity (32). Mice were allowed to eat and drink ad libitum. At various times after infection, mice were sacrificed, and organs were removed. Organ homogenates were prepared as previously described (16) and assayed for infectivity by plaque assay. Pancreatic tissues, fixed with Bouin's solution (Sigma-Aldrich, St. Louis, Mo.), were processed for routine histology, followed by staining with hematoxylin and

* Corresponding author. Mailing address: Wadsworth Center, New York State Department of Health, 120 New Scotland Ave., Albany, NY 12208. Phone: (518) 474-8634. Fax: (518) 402-4773. E-mail: arlene.ramsingh@wadsworth.org.

† Supplemental material for this article may be found at http://jvi.asm.org/.

‡ Present address: Ordway Research Institute, Albany, NY 12208.

eosin. All animal procedures were approved by the Institutional Animal Care and Use Committee of the Wadsworth Center.

Immunohistochemistry. Immunohistochemistry was carried out with modified standard protocols. Briefly, tissue sections were deparaffinized in xylene and rehydrated in ethanol and deionized water. An antigen retrieval step consisting of boiling in 10 mM citric acid–10 mM sodium citrate for 10 min in a microwave oven (540 W), followed by cooling to room temperature, allowed increased binding of the primary antibodies to their antigens. Tissue sections were incubated with the primary antibody, horse anti-type B4 Coxsackie JVB (National Institute of Allergy and Infectious Disease, Bethesda, Md.) or monoclonal anti-mouse proliferating cell nuclear antigen (PCNA) (Sigma) for 30 min at room temperature. After washing three times in phosphate-buffered saline, pH 7.0, sections were incubated with a secondary antibody, biotinylated goat anti-horse immunoglobulin G (Vector Laboratories) or biotinylated goat anti-mouse immunoglobulin G (Sigma). Bound biotinylated antibody was detected with streptavidin-peroxidase and 3,3-diaminobenzidine (Dako Ark kit; Dako Corp., Carpinteria, Calif.), which gives a brown precipitate. Samples were counterstained with hematoxylin. In negative controls, the primary antibody was omitted.

Analysis of mitotically active cells. Cells committed to division express PCNA during the G_1 and S phases of the cell cycle (4). Pancreatic cells committed to division were identified by immunohistochemistry with an anti-PCNA antibody. For each time point, organs from three mice were harvested and analyzed. Digital images of tissue sections were taken at an original magnification of ×234 and displayed in Adobe Photoshop. To determine the percentage of mitotically active acinar cells, PCNA-positive cells were counted and divided by the total number of acinar cells in each of three nonoverlapping fields per tissue section. To determine the percentage of cells within ducts and islets that were mitotically active, cells within 6 to 12 ducts and 6 to 12 islets per tissue section were counted.

Isolation of pancreatic RNA. Pancreas from CVB4-V- and CVB4-P-infected mice were harvested at 4, 5, and 6 days postinfection. This time interval was chosen because the pancreas is already "committed" to regeneration during CVB4-P infection and to extensive destruction during CVB4-V infection. Pancreas from uninfected mice served as controls. At each time point, organs were collected from six mice and pooled. Total cellular RNA was isolated with a modification of the procedure described by McMaster et al. (24). Briefly, organs were flash frozen on dry ice and homogenized in 5 M guanidine thiocyanate (Fluka Chemical Corp., Ronkonkoma, N.Y.)–25 mM EDTA–50 mM Tris (pH 7.4)–8% β-2 mercaptoethanol. Total RNA was precipitated, resuspended in 6 M guanidine hydrochloride–25 mM EDTA–10 mM β-2 mercaptoethanol, and precipitated again. This step was repeated, and the final pellet was resuspended in 75 mM NaCl–25 mM EDTA–0.5% sodium dodecyl sulfate. After extraction with an equal volume of phenol-chloroform (1:1), the aqueous phase was adjusted to 0.3 M ammonium acetate. RNA was again precipitated and resuspended in sterile water. RNA samples were digested with RQ1 RNase-free DNase (Promega, Madison, Wis.) and purified with the RNeasy kit (Qiagen Inc., Valencia, Calif.). RNA integrity was verified by agarose gel electrophoresis, and RNA quality was assessed by reverse transcription-PCR. RNA samples from CVB4-P-infected mice were pooled, and RNA samples from CVB4-V-infected mice were pooled.

Gene expression analysis. Six RNA preparations representing two independent samples for CVB4-P (4, 5, and 6 days postinfection), CVB4-V (4, 5, and 6 days postinfection), and uninfected controls were used. Pancreatic cRNA was prepared according to standard protocols and hybridized to high-density oligonucleotide arrays (Affymetrix MG-U74Av2 mouse GeneChips). Briefly, 7 μg of total RNA was used to generate first-strand cDNA with a T7-linked oligo(dT) primer. After second-strand synthesis, in vitro transcription was performed with biotinylated UTP and CTP.

The standard protocol was used to hybridize, wash, stain, and scan the arrays. A detailed description of procedures is available at www.affymetrix.com/support/technical/manual/expression_manual.affx. The oligonucleotide arrays contained 12,488 probes, of which 9,721 are known genes, 1,714 are Riken cDNAs, 529 are expressed sequence tags (ESTs), 480 have no annotation, and 44 are controls. The 9,721 probes interrogate the expression of 7,087 unique genes.

RESULTS

CVB4-induced pancreatic inflammatory disease. Pathological changes occurring during CVB4-P infection are focal and include acinar cell necrosis, degranulation, inflammation, and edema (Fig. 1). Acinar cell necrosis and degranulation occurred early in infection and were followed by inflammation, edema, and tissue damage (Fig. 1C and E). During the inflammatory response, areas of normal acini were evident. Ten days after infection, inflammation subsided, and the exocrine pancreas was repaired. At this time, the pancreas appeared indistinguishable from those of uninfected mice.

During the first 2 days of infection with CVB4-V, extensive degranulation of the acinar cells was accompanied by inflammation of the exocrine tissues. By 4 days of infection, there was widespread acinar cell necrosis (Fig. 1D), followed by complete loss of acinar cells, 6 days after infection (Fig. 1F). By 14 days after infection, a mild inflammatory infiltrate was evident, along with numerous tubular/ductular structures in a loose, connective matrix (Fig. 1H). The chronic phase of disease, defined as prolonged tissue damage in the absence of infectious virus, is characterized by the sustained presence of inflammatory infiltrates, tubular and ductular structures (acinoductular metaplasia), fibrosis, and fat replacement. Pancreatic ducts and islets during infection with either variant appeared unchanged.

CVB4 replicates in pancreatic acinar cells. To determine whether viral replication influenced the development of acute and chronic diseases, a comparative assessment of replication for both CVB4-V and CVB4-P was done. Overall viral replication in the pancreas was assessed by measuring infectious virus in pancreatic homogenates at various times after infection (Fig. 2A). Although 200-fold less of the CVB4-V variant was used to infect mice, CVB4-V replicated to higher titers than the CVB4-P variant. For both variants, maximal viral titers were observed 2 days after infection and infectious virus was cleared by 10 days for CVB4-P and by 14 days for CVB4-V.

Given that CVB4-V replicated to higher levels than CVB4-P and was associated with more extensive tissue damage, we examined whether increased viral replication correlated with an expanded cellular tropism in the pancreas. Pancreatic tissues were harvested at the peak of viral replication (2 days postinfection), and infected cells were identified by immunohistochemistry with a horse anti-CVB4 antibody. During CVB4-P infection, viral antigen was localized to small, focal areas of acinar cells (Fig. 2B). CVB4-P-infected acinar cells displayed characteristics of apoptotic cells, including a rounded shape, intensely eosinophilic cytoplasm, and dense nuclear chromatin (Fig. 2B, inset). Except for the presence of focal, apoptotic cells, the pancreas appeared essentially normal when CVB4-P replication was maximal. During CVB4-V infection, viral antigen was present in acinar cells throughout the exocrine pancreas (Fig. 2C). As was observed during CVB4-P infection, some CVB4-V-infected acinar cells displayed characteristics of apoptotic cells. A key difference between CVB4-P and CVB4-V infections is that during peak viral replication (2 days postinfection), CVB4-V-infected acinar cells underwent extensive degranulation which correlated with an early inflammatory response, while CVB4-P-infected tissues appeared essentially normal. Viral antigen was not detected in islet or duct cells. The data show that although both viruses were tropic for pancreatic acinar cells, CVB4-P caused a focal infection, while CVB4-V caused a generalized infection.

Acinar cells participate in pancreatic regeneration after CVB4 infection. To determine if pancreatic repair observed during CVB4-P infection is the result of a regenerative process,

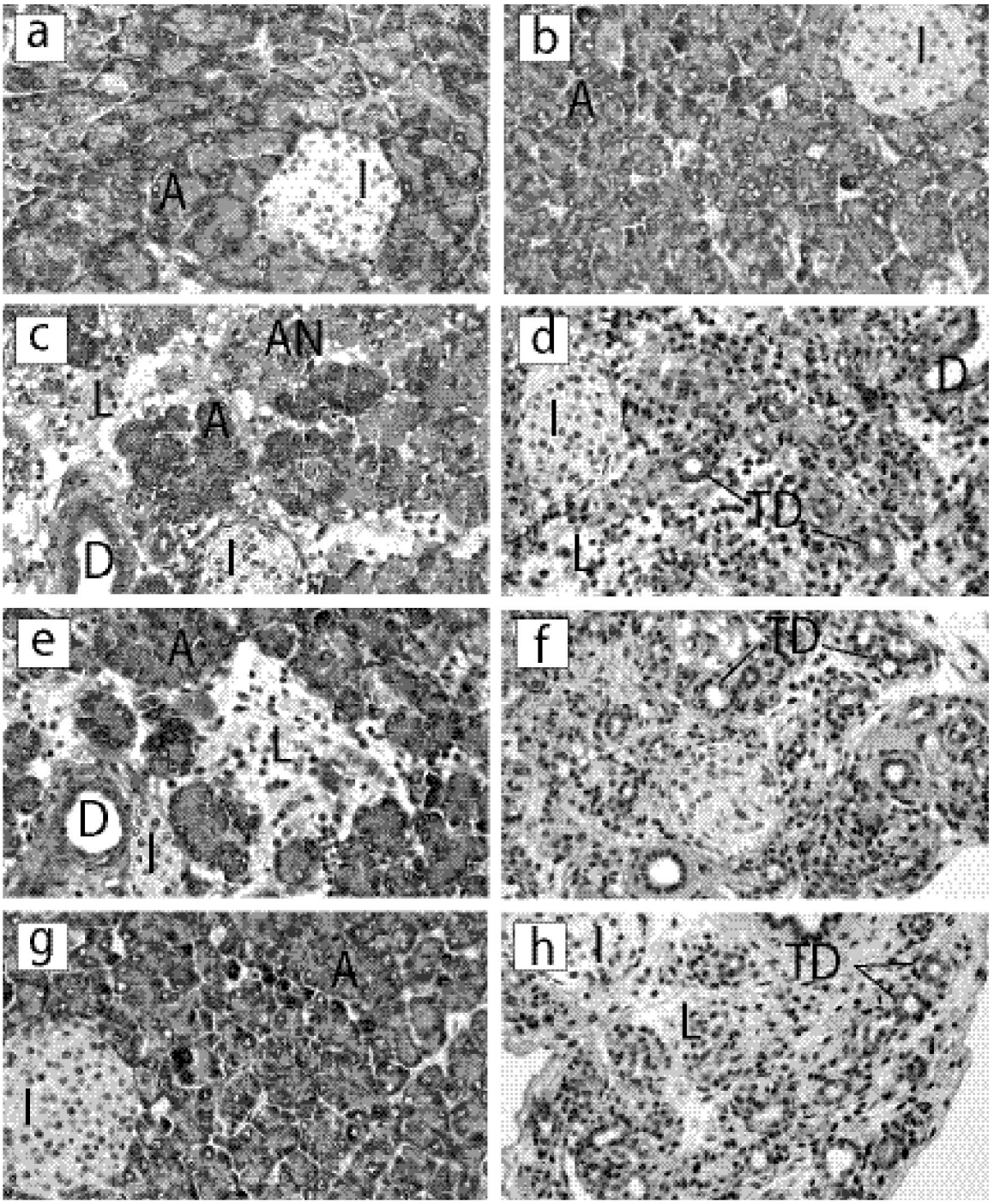

FIG. 1. Histopathology of pancreatic tissues from CVB4-infected mice. Organs were harvested at 4, 6, or 14 days after infection with either CVB4-P or CVB4-V, processed for routine histology, and stained with hematoxylin and eosin. (a and b) Uninfected; (c) CVB4-P, 4 days postinfection; (d) CVB4-V, 4 days postinfection; (e) CVB4-P, 6 days postinfection; (f) CVB4-V, 6 days postinfection; (g) CVB4-P, 14 days postinfection; (h) CVB4-V, 14 days postinfection. A, acini; I, islets of Langerhans; L, lymphocytic infiltrate; AN, acinar cell necrosis; D, pancreatic duct; TD, tubular/ductular structures. Magnification, ×234.

the mitotic activity of pancreatic cells was monitored by immunohistochemistry with an antibody specific for PCNA. Mitotic activity was corroborated by monitoring the incorporation of 5-bromo-2′-deoxyuridine (data not shown). The identity of cells engaged in mitotic activity was confirmed in a double-labeling experiment with anti-PCNA and an exocrine-specific marker, amylase (data not shown). Given that CVB4-P infection results in focal damage to the exocrine pancreas, we examined mitotically active cells in regions of tissue that showed different amounts of damage (none, mild, and severe). Pancreatic damage was observed from 4 to 8 days after infection and coincided with the inflammatory response (Fig. 1 C and E).

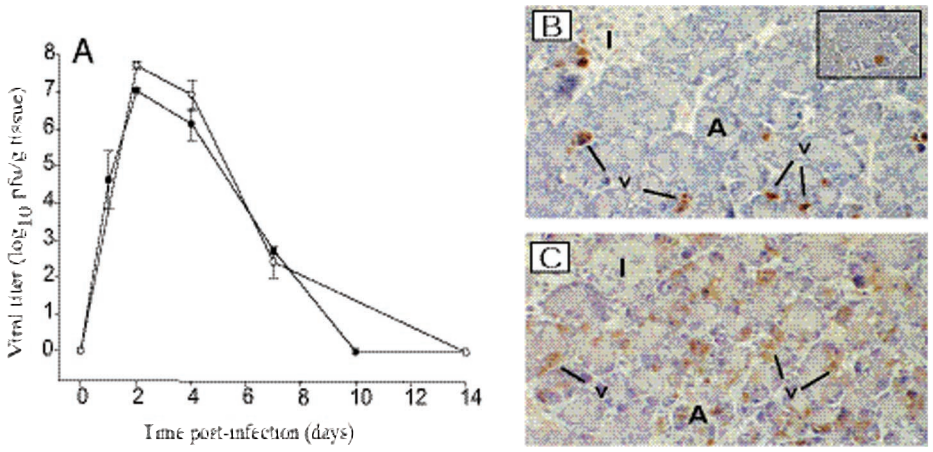

FIG. 2. CVB4 replication in the pancreas. (A) Kinetics of replication in the pancreas of mice infected with CVB4-P (solid circles) and CVB4-V (open circles). Organs harvested at various times after infection were assayed for viral infectivity by plaque assay. Three organs were assayed at each time point. Mean values and standard deviations are shown. (B) CVB4-P causes a focal infection of pancreatic acinar cells. Infected cells were identified by immunohistochemistry with an anticoxsackievirus antibody. Virus-infected cells appear apoptotic (inset; magnification, ×1,170). (C) CVB4-V causes a generalized infection of pancreatic acinar cells. Magnification, ×234. A, acini; I, islets of Langerhans; v, virus.

CVB4-P infection caused a significant increase in the number of mitotically active acinar cells but not of islet or ductal cells. In uninfected mice, less than 1% of acinar cells, 2.7% of islet cells, and 11.1% of ductal cells were mitotically active. Overall acinar cell division increased 4 days after CVB4-P infection, peaked at 8 days, and returned to baseline levels at 10 days, when the exocrine pancreas had fully repaired (Fig. 3A). Acinar cells that were positive for PCNA contained morphologically normal nuclei (Fig. 3B and C). The percentage of mitotically active acinar cells was greatest in severely damaged regions of the exocrine pancreas and peaked 8 days after infection.

A summary of the events occurring during CVB4-P and CVB4-V infections is depicted in Fig. 4. CVB4-P-induced pancreatic inflammatory disease is resolved when infectious virus is cleared (within 10 days of infection). Exocrine pancreatic damage is focal and is repaired via a regenerative process in which acinar cells participate. CVB4-V-induced pancreatic inflammatory disease progresses to chronic disease after infectious virus is cleared (within 14 days of infection). The chronic

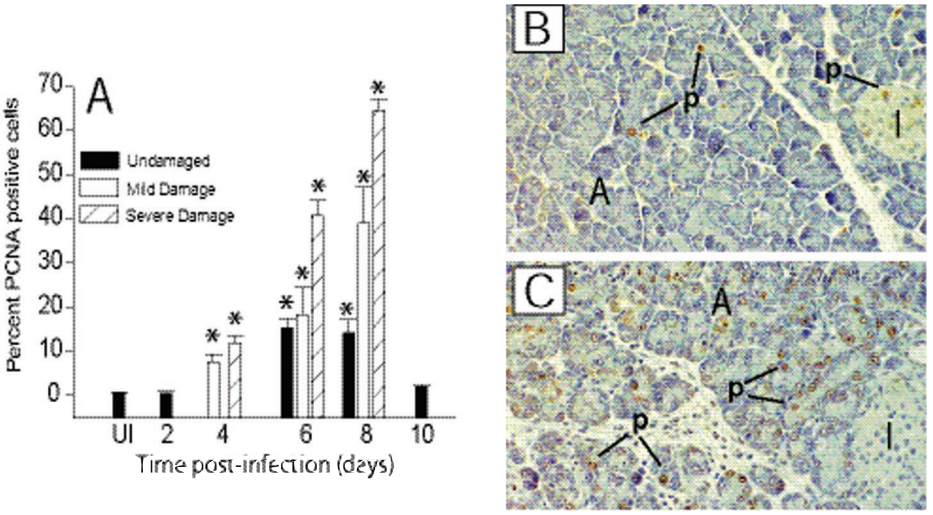

FIG. 3. Mitotically active acinar cells in the exocrine pancreas of CVB4-P-infected mice. (A) Semiquantitative assessment of mitotically active (PCNA-positive) acinar cells during CVB4-P infection. Dividing acinar cells in regions of tissue that appeared undamaged, mildly damaged, and severely damaged were counted. For each organ, mitotically active cells in three nonoverlapping fields were scored for each category of damage. Three organs were evaluated at each time point. Mean values and standard deviations are shown. Statistical analysis was performed by analysis of variance. Statistically significant differences ($P < 0.001$) between uninfected and CVB4-P-infected tissues are denoted by asterisks. (B) Immunohistochemical staining of an uninfected pancreas with an anti-PCNA antibody. PCNA staining is restricted to a few acinar and islet cells. (C) Immunohistochemical staining of a pancreas 8 days after infection with CVB4-P. The number of PCNA-positive acinar cells increased after CVB4-P infection. A, acini; p, PCNA positive; I, islet of Langerhans. Magnification, ×234.

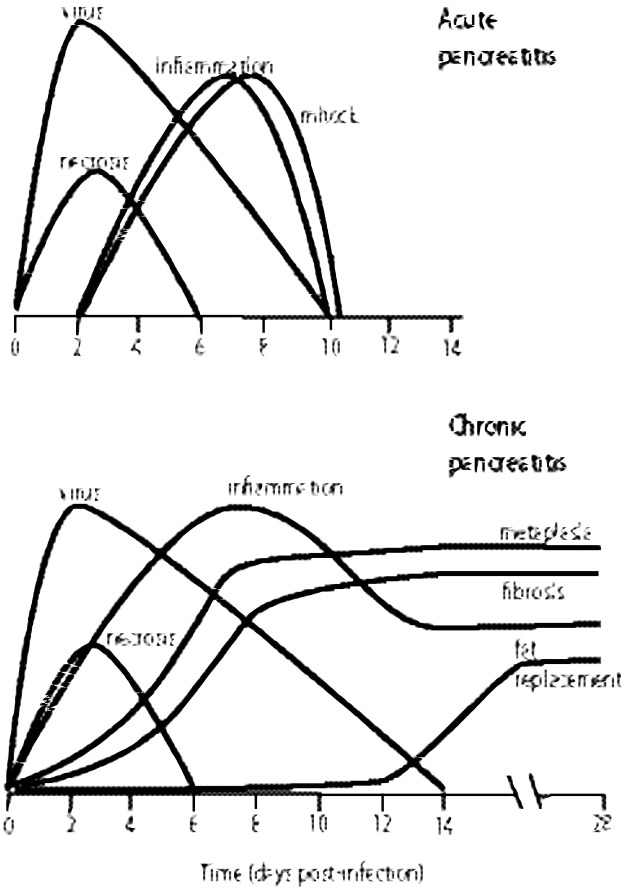

FIG. 4. Characteristic features of CVB4-induced acute and chronic pancreatitis. Gene expression was analyzed 4 to 6 days after infection, when viral titers were decreasing. The time interval coincided with the presence of inflammatory cells and mitotically active acinar cells for CVB4-P and with inflammation, acinoductular metaplasia, and fibrosis for CVB4-V.

stage of disease is characterized by the sustained presence of inflammatory infiltrates, tubular/ductular structures, fibrosis, and fat replacement.

Microarray data analysis. This study was undertaken to identify genes whose expression correlated with disease resolution or disease progression. The approach was to examine global gene expression in models of regeneration (CVB4-P infection), chronic tissue damage (CVB4-V infection), and uninfected controls with microarrays. Ideally, gene expression would have been evaluated at multiple, individual time points after infection. However, due to cost limitations, these studies focused on gene expression in pooled pancreatic samples harvested at multiple days (4, 5, and 6) after infection. This time interval was chosen because the repair process, as evidenced by an overall increase in acinar cell division (Fig. 3A), was under way in CVB4-P infection. At the same time, characteristic features of chronic pancreatitis (acinoductular metaplasia and fibrosis) were apparent in CVB4-V infection (Fig. 4). The assumption was that differential gene expression during this time interval would allow the identification of genes involved in disease resolution and disease progression.

The focus of the study was the identification of genes whose expression was significantly altered between CVB4-P and CVB4-V infections and between uninfected and infected samples. Genes whose expression was altered between uninfected and infected samples but was similar between CVB4-P and CVB4-V infections represent common responses to infection and are not discussed in this report. The initial analysis compared gene expression in CVB4-P (P) and CVB4-V (V) infections and identified two subsets of genes ($V > P$; $P > V$). A subsequent analysis compared expression of the two subsets with that observed in the uninfected (UI) control sample and generated four groups ($V > P > UI$; $V > UI > P$; $P > V > UI$; $P > UI > V$).

Data analysis focused on normalization to correct for variation attributed to differences between chip intensities (manufacturing variation) and experimental RNA preparations, variance correction for replicate samples, and differential gene expression in CVB4-P-infected, CVB4-V-infected, and uninfected samples. Image data from the three replicate experiments were preprocessed via log scale robust multiarray analysis (RMA) as described (18). (Data from Affymetrix.CEL files were used as input for the RMA analysis.) This technique considers the perfect-match (2) probe intensities on the chips and subjects them to normalization and mismatch-based background correction (6, 19). Normalization to correct for variation attributed to manufacturing variation and experimental RNA preparations was accomplished with quantile normalization. Background correction corrects the intensities for nonspecific binding and optical noise and is based on a mixture of an exponential for the chip-specific background and a normal distribution for probe intensities. RMA values are used for all ensuing analyses. Data obtained from replicate samples were consistent because uncorrected and variance-corrected analyses identified essentially the same set of probes.

To identify genes whose expression was significantly different during CVB4-P and CVB4-V infections, a robust self-critical estimation procedure (31), with a criticism coefficient of 0.6, was used to estimate five underlying normal distribution parameters. This procedure is highly resistant to the presence of outliers and provides the boundaries for elliptical regions enclosing specified amounts (50, 85, 97.5, and 99.9%) of the underlying normal distribution. Comparison of these elliptical regions with the corresponding regions actually observed in the microarray data provides a means to assess the goodness of fit of the underlying normal distribution. In addition, the comparison allows us to identify, in the extreme regions, altered probes whose expression levels exceed those that are theoretically expected. Figure 5 shows the results of the microarray experiment displayed as a log-scaled plot of abundances (duplicate averaged CVB4-P and CVB4-V intensities) versus differences (duplicate averaged CVB4-P) − (duplicate averaged CVB4-V). Examination of Fig. 5 reveals close correspondence between the 50 and 85% ellipsoidal regions, which are expected to enclose 6,244 and 4,370 probes, with the areas actually occupied by 50% (tan) and 85% (turquoise) of the data: 4.6% (290 of 6,244) are outside the 50% ellipse, and 10.5% (457 of 4,370) are outside the 85% ellipse. The 97.5% ellipse demonstrates clear nonnormality, with 45.4% (709 of 1,561) of the data exceeding its boundary and an absence of low-abundance probes. This trend continues in the 99.9% region, where all of the data (red) are outside the 99.9% ellipse.

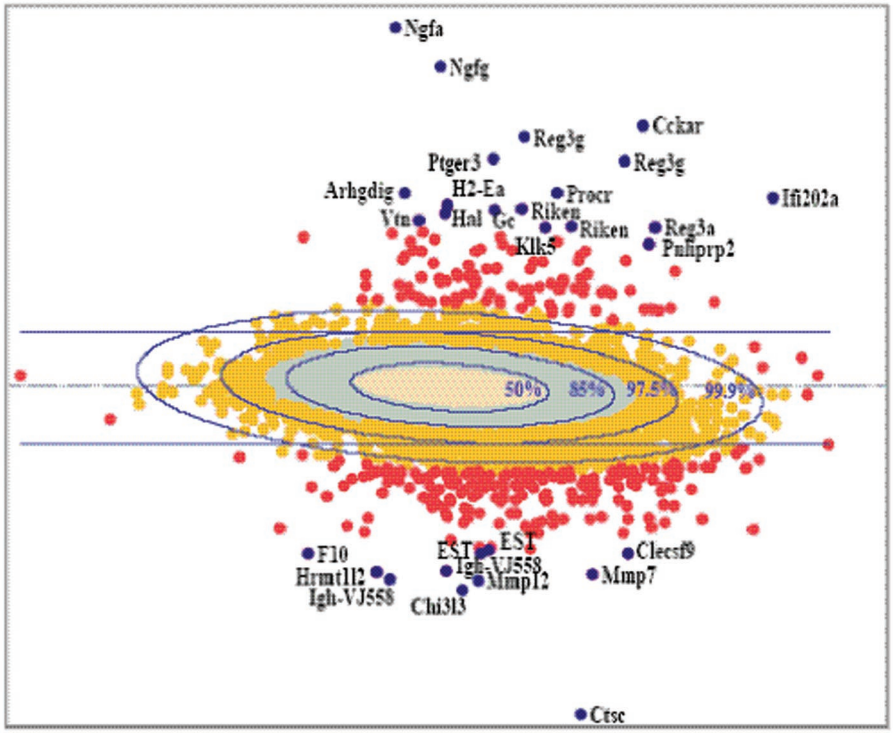

FIG. 5. Summary of gene expression data for CVB4-P and CVB4-V. Results are displayed as a log-scaled plot of differences [(duplicate averaged CVB4-P) − (duplicate averaged CVB4-V)] versus abundances (duplicate averaged CVB4-P and CVB4-V intensities). Ellipses denote predicted levels of significance. The data set is shown in five colors to denote different P values. Blue, $P < 0.01$; red, $P = 0.01$; gold, $P = 0.025$; turquoise, $P = 0.15$; and tan, $P = 0.5$. The most significant outliers (blue genes) are labeled individually.

The results suggest that the robust estimation has located an underlying Gaussian distribution providing a nearly perfect fit to the central 85% of the data, except for some residual influence due to the large number of probes with altered expression. The estimates further determine that 45% of the probes in the next 12.5 and 100% of the probes in the final 2.5% of the data are unlikely to have arisen by chance. Since the focus of this study is the identification of genes that are significantly different during CVB4-P and CVB4-V infections, significance thresholds tangent to the extreme values of the 97.5% ellipse were established to delineate a set of probes significant at least at the 2.5% level ($P = 0.025$). This resulted in the identification of 222 probes which were expressed at higher levels in CVB4-P than in CVB4-V infection (above the top line in Fig. 5) and 622 probes which were expressed at higher levels in CVB4-V than in CVB4-P infection (below the bottom line in Fig. 5). Recently, a new method based on controlling the positive false discovery rate has been proposed for assessing the number of probes to call positive (39). Applying this technique in the current data set suggests that if 844 probes ($P = 0.025$) are called significant, only about 6% (54 probes) will be false-positives.

Global gene expression during disease resolution and disease progression. The group of 222 probes whose expression was greater in CVB4-P than in CVB4-V infection contained 169 unique known genes, of which 129 showed increased expression in CVB4-P infection compared to the uninfected control. The group of 622 probes whose expression was greater in CVB4-V than in CVB4-P infection contained 338 unique known genes, of which 336 showed increased expression in CVB4-V infection compared to the uninfected control. Based on function, genes were assigned to specific categories (Fig. 6) and interpreted in the context of events known to be occurring in the pancreas. Genes with multiple functions were assigned to more than one category.

Comparison of expression profiles of infected and uninfected samples showed that more genes (additional 22%) were expressed during CVB4-P than in CVB4-V infection. For the subset of genes whose expression was increased during both infections, 84% (Fig. 6, hatched bars) were expressed at higher levels during CVB4-V infection and 16% (Fig. 6, grey bars) were expressed at higher levels during CVB4-P infection. Functional categorization of these genes is presented in supplemental Tables S1 to S7. CVB4-P-specific genes (Fig. 6, open bars) are genes whose expression was increased during CVB4-P infection and depressed during CVB4-V infection, relative to the uninfected sample (supplemental Table S8). Similarly, CVB4-V-specific genes (Fig. 6, black bars) are genes whose expression was increased during CVB4-V infection and depressed during CVB4-P infection, relative to the uninfected sample (supplemental Table S9).

CVB4-P-specific genes are more numerous than CVB4-V-specific genes and are observed in all categories. The cell growth and development category contains the highest number of CVB4-P- specific genes, which include genes expressed during embryonic development, growth and differentiation, apoptosis, and angiogenesis. CVB4-V-specific genes are observed in all categories except functional pancreas, which contains

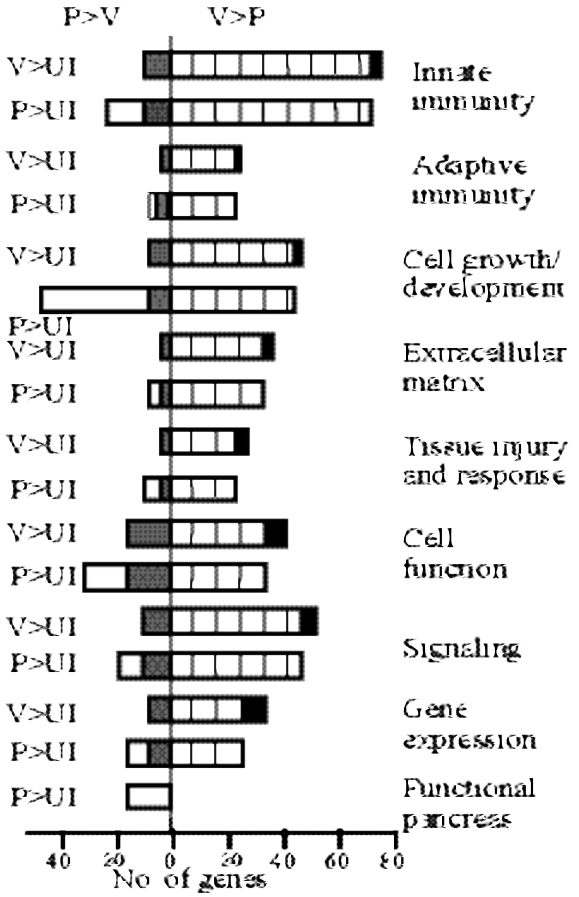

FIG. 6. Functional groupings of genes whose expression was increased during CVB4 infection relative to uninfected controls. Open bars, CVB4-P-specific genes; black bars, CVB4-V-specific genes; grey bars, gene expression greater during CVB4-P than CVB4-V infection; hatched bars, gene expression greater during CVB4-V- than CVB4-P infection. V, CVB4-V; P, CVB4-P; UI, uninfected.

only CVB4-P-specific genes. This subset of genes encodes a variety of pancreatic enzymes and proteins involved in secretion. The presence of only CVB4-P-specific genes in this category validates the results of the study and serves as a positive, internal control because the pancreas is restored after CVB4-P but not CVB4-V infection.

DISCUSSION

This study focused on the genetic events underlying the two outcomes of CVB4-induced acute pancreatitis, disease resolution and progression to chronic pancreatitis. Infection with the nonvirulent variant, CVB4-P, caused transient damage to the exocrine pancreas which was eventually repaired. Pancreatic regeneration has been studied extensively in many different experimental models, and the resulting data have generated much controversy. One view is that the pancreatic duct system contains precursor cells that can give rise to new acinar cells, duct cells, and islet cells (8, 33, 41). Another view is that each differentiated cell type is able to restore its own population after cell loss (13). In a rat model of partial pancreatectomy, these two views were reconciled when two pathways of pancreatic regeneration were shown to exist (7). In one pathway, existing, differentiated exocrine and endocrine cells replicate. In the other pathway, ductal epithelium proliferates and differentiates to form new pancreatic lobules. Depending on the experimental model, pancreatic regeneration appears to occur via different pathways. We have shown that during the repair process, acinar cells underwent increased cell division. Our data provide support for the participation of differentiated acinar cells in pancreatic regeneration.

Under homeostatic conditions, a balance between apoptosis and cell division is needed to maintain healthy tissues. If tissues are to be repaired subsequent to injury, the balance must shift to favor cell division. During repair of the pancreas, we observed an increase in the expression of genes associated with cell growth (*Vnn1*, *Egf*, *Nupr1*, and *Arg2*) (22, 23, 27, 28) and with the inhibition of apoptosis (*Birc4, Reg3a*, *Reg3g*, and *Pap*) (10, 38). The shift towards cell growth and inhibition of apoptosis coincided with increased expression of genes associated with angiogenesis (*Ang, Hpn, Klks*, and *Serpins*) (3, 14, 37). The coincident expression of genes associated with cell growth and angiogenesis suggests a relationship between these two processes. A recent study showed that in a model of diabetes, bone marrow transplantation is able to lower blood glucose levels and bone marrow cells become vascular endothelial cells and not insulin-producing beta cells (17). The authors speculate that new blood vessels secrete growth and differentiation factors which induce β-cell regeneration from resident pancreatic cells. Similar events may be occurring in our model of exocrine pancreatic growth.

During CVB4-P infection, there is an increase in the expression of embryonic markers (*Nes*, *Ngfa*, *Ngfg*, *Sel1h*, and *Mgat1*). This group of five genes is specifically downregulated during CVB4-V infection, suggesting that they are key players in pancreatic regeneration. Nestin-positive cells are pluripotent, able to differentiate into both exocrine and endocrine cells (1, 43). Nestin may be a marker of pancreatic stem cells. *Ngfa*, *Ngfg*, and *Mgat1* are also expressed in the developing pancreas and may participate in morphogenesis (20, 26, 30, 40). *Sel1h* downregulates the Notch system, which is involved in regulating the balance between cell differentiation and stem cell proliferation (5). The presence of these embryonic markers in the regenerating pancreas suggests that stem cells are present or that pancreatic cells are undergoing dedifferentiation and expressing embryonic markers. We hypothesize that during CVB4-P infection, pancreatic stem cells responding to growth and differentiation signals (from new blood vessels?) differentiate into acinar cells, which continue to divide and repopulate the exocrine pancreas.

The innate and adaptive immune responses occurring during CVB4-P and CVB4-V infections appear to be both quantitatively and qualitatively different. Markers of activated macrophages and lymphocytes are expressed at higher levels during CVB4-V than CVB4-P infections (supplemental Table S4), suggesting that immune responses are stronger during CVB4-V infection. The overexpression of *Arg1*, *Cxcl9*, *Cxcl10*, *Ccl3*, *Ccl4*, and *Ccl5* during CVB4-V infection indicates the presence of classically activated (M1) macrophages, while diminished expression of these genes along with overexpression of *Arg2* during CVB4-P infection indicates the presence of alternatively activated (M2) macrophages (23). Macrophage polariza-

tion is not absolute and is generally considered a conceptual framework for a continuum of functional states (23). As a result, macrophage polarization may be viewed as more skewed toward the M1 phenotype during CVB4-V infection and toward the M2 phenotype during CVB4-P infection. Polarization of macrophages may influence T helper cell development (29). M1 macrophages affect Th1 development, resulting in activated CD8 T cells and macrophages, while M2 macrophages influence Th2 development, resulting in B-cell responses. The increased expression of B-cell markers (*Igh-VS107*, *Pigr*, *Igj*, and *Igk-V8*) during CVB4-P infection indicates that T helper cell development is skewed toward a Th2 phenotype.

The kinetics of the inflammatory response and acinar cell division coincide during CVB4-P infection (Fig. 4), suggesting a link between immune responses and pancreatic cell growth. In tissues undergoing repair, mechanisms for overriding apoptosis and growth arrest must exist. Since tissue repair occurs subsequent to damage and an ensuing inflammatory response, it is conceivable that immune mediators (cytokines and chemokines) play a role in the process of cell growth. Evidence supporting a link between inflammatory responses and cell growth comes from studies of macrophage migration inhibitory factor. Migration inhibitory factor has been shown to suppress p53-mediated growth arrest and apoptosis (15). Our working hypothesis is that during CVB4-P infection, the inflammatory milieu provides signals to newly, differentiated and existing, residual acinar cells to overcome the controls favoring growth arrest and apoptosis, resulting in a temporary shift towards proliferation. As the inflammatory response wanes, signals favoring proliferation are removed, allowing the balance between cell growth and apoptosis to be restored.

This study is a "snapshot" of the genetic events underlying acute and chronic inflammatory diseases of the pancreas and reflects the complexity of the disease process. Our analysis does not take into account the influence of events occurring in other organs and tissues that may contribute to the beneficial or detrimental outcomes after infection. Furthermore, gene expression profiles reflect transcriptional events occurring in the whole pancreas since cRNA transcripts were prepared from entire organs and represent a mixed cell population of uninfected cells, infected cells, and inflammatory cells. The use of pooled organs harvested at multiple time points is expected to affect relative levels of gene expression. For example, relative expression will be underrepresented for those genes whose expression increases transiently during the time interval studied.

The expression map of CVB4-V-induced pancreatitis provides insight into the genetic events underlying specific features of this disease. The genetic data show increased expression of genes favoring apoptosis, acinoductular metaplasia, fibrosis, remodeling of the extracellular matrix, and extracellular matrix formation (supplemental Tables S1 and S2). The data suggest that subsequent to CVB4-V-induced tissue injury, the balance shifts away from acinar cell proliferation to favor apoptosis and extracellular matrix formation and remodeling. The overexpression of genes associated with transforming growth factor beta signaling (supplemental Table S2) suggests that the transforming growth factor beta signaling pathway is involved in favoring apoptosis and fibrosis.

The expression map of CVB4-V-induced pancreatitis also provides insight into the failure of the pancreas to repair subsequent to CVB4-V infection. According to our working model, acinar cells respond to signals (possibly from new blood vessels) that favor proliferation. During CVB4-V infection, these signals may be absent or diminished. If growth and differentiation signals are derived from new blood vessels, then one would predict that angiogenesis is diminished during CVB4-V infection. The gene expression data indicate a decreased angiogenic response (supplemental Table S1) which may prevent the differentiation of pancreatic stem cells into acinar cells. Compounding the problem is the survival of only a few, residual acinar cells after CVB4-V infection. The genetic data also indicate qualitative differences in the inflammatory milieu during CVB4-V (M1 and Th1) and CVB4-P (M2 and Th2) infections. An extension of our model is that diminished angiogenic responses coupled with the M1 and Th1 milieu favors apoptosis of acinar cells along with growth and remodeling of the extracellular matrix, resulting in fibrosis. Similarly, a heightened angiogenic response coupled with the M2 and Th2 milieu favors acinar cell proliferation. If true, then a prediction of the model is that modulation of either the angiogenic or immune response during CVB4-V infection would be beneficial. We have recently shown that immune modulation via cytokine (interleukin-12) administration protects the exocrine pancreas and prevents morbidity and mortality during CVB4-V infection (32). Since the inflammatory milieu induced by CVB4 may influence disease progression, future studies will examine global gene expression early in the infection process to identify candidate genes that influence the outcome of infection.

ACKNOWLEDGMENTS

This work was supported by Public Health Service grant AI52705 from the National Institutes of Health and by the American Heart Association.

We thank the staff of the Department of Pathology for processing tissue samples for histology. The microarray experiments were done by the Microarray Core Facility. Analysis of the gene expression data was done by the Computational Molecular Biology and Statistics Core. The secretarial assistance of Maryellen Carl is greatly appreciated.

REFERENCES

1. **Abraham, E. J., C. A. Leech, J. C. Lin, H. Zulewski, and J. F. Habener.** 2002. Insulinotropic hormone glucagon-like peptide-1 differentiation of human pancreatic islet-derived progenitor cells into insulin-producing cells. Endocrinology **143:**3152–3161.
2. **Affymetrix.** 2001. Microarray suite user guide, version 5. Affymetrix, Santa Clara, Calif.
3. **Aimes, R. T., A. Zijlstra, J. D. Hooper, S. M. Ogbourne, M. L. Sit, S. Fuchs, D. C. Gotley, J. P. Quigley, and T. M. Antalis.** 2003. Endothelial cell serine proteases expressed during vascular morphogenesis and angiogenesis. Thromb. Haemost. **89:**561–572.
4. **Alberts, B., D. Bray, J. Lewis, M. Raff, K. Roberts, and J. D. Watson.** 1995. Molecular biology of the cell. Garland Publishing, New York, N.Y.
5. **Artavanis-Tsakonas, S., M. D. Rand, and R. J. Lake.** 1999. Notch signaling: cell fate control and signal integration in development. Science **284:**770–776.
6. **Bolstad, B. M., R. A. Irizarry, M. Strand, and T. P. Speed.** 2003. A comparison of normalization methods for high density oligonucleotide array data based on variance and bias. Bioinformatics **19:**185–193.
7. **Bonner-Weir, S., L. A. Baxter, G. T. Schuppin, and F. E. Smith.** 1993. A second pathway for regeneration of adult exocrine and endocrine pancreas. A possible recapitulation of embryonic development. Diabetes **42:**1715–1720.
8. **Bonner-Weir, S., M. Taneja, G. C. Weir, K. Tatarkiewicz, K. H. Song, A. Sharma, and J. J. O'Neil.** 2000. In vitro cultivation of human islets from expanded ductal tissue. Proc. Natl. Acad. Sci. USA **97:**7999–8004.
9. **Bradley, E. L.** 1994. Acute pancreatitis: diagnosis and therapy. Raven Press, New York, N.Y.

10. **Bratton, S. B., J. Lewis, M. Butterworth, C. S. Duckett, and G. M. Cohen.** 2002. XIAP inhibition of caspase-3 preserves its association with the Apaf-1 apoptosome and prevents. Cell Death Differ. **9:**881–892.
11. **Caggana, M., P. Chan, and A. Ramsingh.** 1993. Identification of a single amino acid residue in the capsid protein VP1 of coxsackievirus B4 that determines the virulent phenotype. J. Virol. **67:**4797–4803.
12. **Chapman, N. M., A. I. Ramsingh, and S. Tracy.** 1997. Genetics of coxsackievirus virulence. Curr. Top. Microbiol. Immunol. **223:**227–258.
13. **Elsasser, H. P., G. Adler, and H. F. Kern.** 1986. Time course and cellular source of pancreatic regeneration following acute pancreatitis in the rat. Pancreas **1:**421–429.
14. **Emanueli, C., and P. Madeddu.** 2002. Renin-angiotensin and kallikrein-kinin systems coordinately modulate angiogenesis. Hypertension **39:**e29.
15. **Fingerle-Rowson, G., O. Petrenko, C. N. Metz, T. G. Forsthuber, R. Mitchell, R. Huss, U. Moll, W. Muller, and R. Bucala.** 2003. The p53-dependent effects of macrophage migration inhibitory factor revealed by gene targeting. Proc. Natl. Acad. Sci. USA **100:**9354–9359.
16. **Halim, S., and A. I. Ramsingh.** 2000. A point mutation in VP1 of coxsackievirus B4 alters antigenicity. Virology **269:**86–94.
17. **Hess, D., L. Li, M. Martin, S. Sakano, D. Hill, B. Strutt, S. Thyssen, D. A. Gray, and M. Bhatia.** 2003. Bone marrow-derived stem cells initiate pancreatic regeneration. Nat. Biotechnol. **21:**763–770.
18. **Irizarry, R. A., B. M. Bolstad, F. Collin, L. M. Cope, B. Hobbs, and T. P. Speed.** 2003. Summaries of Affymetrix GeneChip probe level data. Nucleic Acids Res. **31:**E15.
19. **Irizarry, R. A., B. Hobbs, F. Collin, Y. D. Beazer-Barclay, K. J. Antonellis, U. Scherf, and T. P. Speed.** 2003. Exploration, normalization, and summaries of high density oligonucleotide array probe level data. Biostatistics **4:**249–264.
20. **Kanaka-Gantenbein, C., A. Tazi, P. Czernichow, and R. Scharfmann.** 1995. In vivo presence of the high affinity nerve growth factor receptor Trk-A in the rat pancreas: differential localization during pancreatic development. Endocrinology **136:**761–769.
21. **Knowlton, K. U., E. S. Jeon, N. Berkley, R. Wessely, and S. Huber.** 1996. A mutation in the puff region of VP2 attenuates the myocarditic phenotype of an infectious cDNA of the Woodruff variant of coxsackievirus B3. J. Virol. **70:**7811–7818.
22. **Mallo, G. V., F. Fiedler, E. L. Calvo, E. M. Ortiz, S. Vasseur, V. Keim, J. Morisset, and J. L. Iovanna.** 1997. Cloning and expression of the rat p8 cDNA, a new gene activated in pancreas during the acute phase of pancreatitis, pancreatic development, and regeneration, and which promotes cellular growth. J. Biol. Chem. **272:**32360–32369.
23. **Mantovani, A., S. Sozzani, M. Locati, P. Allavena, and A. Sica.** 2002. Macrophage polarization: tumor-associated macrophages as a paradigm for polarized M2 mononuclear phagocytes. Trends Immunol. **23:**549–555.
24. **McMaster, M. T., R. C. Newton, S. K. Dey, and G. K. Andrews.** 1992. Activation and distribution of inflammatory cells in the mouse uterus during the preimplantation period. J. Immunol. **148:**1699–1705.
25. **Mergener, K., and J. Baillie.** 1997. Chronic pancreatitis. Lancet **350:**1379–1385.
26. **Metzler, M., A. Gertz, M. Sarkar, H. Schachter, J. W. Schrader, and J. D. Marth.** 1994. Complex asparagine-linked oligosaccharides are required for morphogenic events during post-implantation development. EMBO J. **13:** 2056–2065.
27. **Michalopoulos, G. K., and M. C. DeFrances.** 1997. Liver regeneration. Science **276:**60–66.
28. **Mills, C. D.** 2001. Macrophage arginine metabolism to ornithine/urea or nitric oxide/citrulline: a life or death issue. Crit. Rev. Immunol. **21:**399–425.
29. **Mills, C. D., K. Kincaid, J. M. Alt, M. J. Heilman, and A. M. Hill.** 2000. M-1/M-2 macrophages and the Th1/Th2 paradigm. J. Immunol. **164:**6166–6173.
30. **Miralles, F., P. Philippe, P. Czernichow, and R. Scharfmann.** 1998. Expression of nerve growth factor and its high-affinity receptor Trk-A in the rat pancreas during embryonic and fetal life. J. Endocrinol. **156:**431–439.
31. **Paulson, A. S. and Delehanty, T. A.** 1983. Sensitivity analysis in experimental design, p. 52–57. *In* K. W. Heiner, R. S. Sacher, and J. W. Wilkinson (ed.), Proceedings of the 14th Symposium on the Interface. Springer Verlag, New York, N.Y.
32. **Potvin, D. M., D. W. Metzger, W. T. Lee, D. N. Collins, and A. I. Ramsingh.** 2003. Exogenous interleukin-12 protects against lethal infection with coxsackievirus B4. J. Virol. **77:**8272–8279.
33. **Ramiya, V. K., M. Maraist, K. E. Arfors, D. A. Schatz, A. B. Peck, and J. G. Cornelius.** 2000. Reversal of insulin-dependent diabetes using islets generated in vitro from pancreatic stem cells. Nat. Med. **6:**278–282.
34. **Ramsingh, A. I., W. T. Lee, D. N. Collins, and L. E. Armstrong.** 1997. Differential recruitment of B and T cells in coxsackievirus B4-induced pancreatitis is influenced by a capsid protein. J. Virol. **71:**8690–8697.
35. **Ramsingh, A. I., W. T. Lee, D. N. Collins, and L. E. Armstrong.** 1999. T cells contribute to disease severity during coxsackievirus B4 infection. J. Virol. **73:**3080–3086.
36. **Schwimmbeck, P. L., S. A. Huber, and H. P. Schultheiss.** 1997. Roles of T cells in coxsackievirus B-induced disease. Curr. Top. Microbiol. Immunol. **223:**283–303.
37. **Shestenko, O. P., S. D. Nikonov, and N. P. Mertvetsov.** 2001. Angiogenin and its role in angiogenesis. Mol. Biol. **35:**294–314.
38. **Simon, M. T., A. Pauloin, G. Normand, H. T. Lieu, H. Mouly, G. Pivert, F. Carnot, J. G. Tralhao, C. Brechot, and L. Christa.** 2003. HIP/PAP stimulates liver regeneration after partial hepatectomy and combines mitogenic and anti-apoptotic functions through the PKA signaling pathway. FASEB J. **17:**1441–1450.
39. **Storey, J. D.** 2002. A direct approach to false discovery rates. J. R. Statist. Soc. B **64:**479–498.
40. **Teitelman, G., Y. Guz, S. Ivkovic, and M. Ehrlich.** 1998. Islet injury induces neurotrophin expression in pancreatic cells and reactive gliosis of peri-islet Schwann cells. J. Neurobiol. **34:**304–318.
41. **Tosh, D., and J. M. Slack.** 2002. How cells change their phenotype. Nat. Rev. Mol. Cell. Biol. **3:**187–194.
42. **Tu, Z. G., N. M. Chapman, G. Hufnagel, S. Tracy, J. R. Romero, W. H. Barry, L. P. Zhao, K. Currey, and B. Shapiro.** 1995. The cardiovirulent phenotype of coxsackievirus B3 is determined at a single site in the genomic 5′ nontranslated region. J. Virol. **69:**4607–4618.
43. **Zulewski, H., E. J. Abraham, M. J. Gerlach, P. B. Daniel, W. Moritz, B. Muller, M. Vallejo, M. K. Thomas, and J. F. Habener.** 2001. Multipotential nestin-positive stem cells isolated from adult pancreatic islets differentiate ex vivo into pancreatic endocrine, exocrine, and hepatic phenotypes. Diabetes **50:**521–533.